Nuclear spectroscopy of ^{24}Na via $(\vec{d}, p)$ and (n, γ) reactions

I. Tomandl,* J. Novák, and V. Burjan
Nuclear Physics Institute, CZ-250 68 Řež, Czech Republic

S. Raman†
Oak Ridge National Laboratory, Oak Ridge, Tennessee 37831, USA

T. von Egidy, H.-F. Wirth, U. Köster, and W. Schauer
Physik Department, Technische Universität München, D-85748 Garching, Germany

J. W. Starner and E. T. Jurney†
Los Alamos National Laboratory, Los Alamos, New Mexico 87545, USA

G. Graw, R. Hertenberger, A. Gollwitzer, B. Valnion, and A. Metz
Sektion Physik, Universität München, D-85748 Garching, Germany
(Received 13 October 2003; published 28 January 2004)

The ^{24}Na nucleus was investigated via $(\vec{d}, p)$ and (n, γ) reactions. Within the range of excitation energy from 0 to 6.3 MeV 75 levels were observed. The angular distribution of partial cross sections and vector analyzing powers for 70 levels were determined within the framework of distorted-wave Born approximation. Of 240 γ transitions assigned to ^{24}Na, 234 were placed in the decay scheme. Based on the extensive (n, γ) data the neutron separation energy was deduced to be 6959.44 ± 0.05 keV. Using spectroscopic information from our $(\vec{d}, p)$ measurement we investigated the role of the direct capture mechanism in the ^{23}Na$(n, \gamma)^{24}$Na reaction.

DOI: 10.1103/PhysRevC.69.014312 PACS number(s): 21.10.Jx, 25.40.Lw, 27.30.+t

I. INTRODUCTION

The ^{24}Na nucleus lies in the *sd* shell where complete shell-model calculations became available. Especially for ^{24}Na a recent publication on the ^{25}Mg$(d, ^3$He$)^{24}$Na reaction [1] demonstrated that all positive parity levels up to 3.6 MeV are well reproduced and that also spectroscopic factors for proton pickup are in agreement with these calculations. Very precise, detailed, and complete nuclear level schemes are required in order to test and confirm shell-model calculations and the corresponding theoretical basis for *sd*-shell nuclei. Consequently, it was the goal of Raman and his co-workers to perform most precise (n, γ) experiments at Los Alamos, combine them with the best other spectroscopic information and construct very accurate, extensive, and consistent level schemes. In this context the following nuclei were studied: ^{15}N [2], ^{20}F [3], ^{25,26,27}Mg [4], ^{29,30,31}Si [5], and ^{33,34,35,37}S [6].

The odd-odd nucleus ^{24}Na has been previously investigated applying a large variety of reactions [7]. The most precise and comprehensive information came from the (n, γ) reaction using Ge detectors and also crystal spectrometers. Early (n, γ) experiments were compiled in 1967 by Bartholomew *et al.* [8]. Later the (n, γ) reaction was measured by Nichol *et al.* [9], Wilson *et al.* [10], Tielens and co-workers [11,12], Hungerford *et al.* [13], Ming *et al.* [14], and Hori *et al.* [15] in Hamilton, Argonne, Petten, Grenoble, Beijing, and Tokyo, respectively. More than 100 γ lines are seen in these studies. These results can be compared with γ data from $(^3$He$, p\gamma)$ [16], $(d, p\gamma)$ [17–19], and $(d, \alpha\gamma)$ [20]. The following transfer reactions were published: (d, p) [21,22], $(d, ^3$He$)$ [1,23], (d, α) [24], $(t, ^3$He$)$ [25], $(^3$He$, p)$ [26,27] and (α, d) [28]. Many experimental l values were deduced from angular distributions of direct reaction ejectiles and helped in determining spins and parities of levels. The (d, α) reaction with polarized deuterons [24] distinguishes between states with natural or unnatural parity, a crucial argument for spin-parity assignments.

In spite of these efforts many ambiguities in the level scheme remained and the completeness was questionable. Therefore, we performed a very precise and sensitive (n, γ) measurement in Los Alamos in order to obtain a complete level scheme containing nearly all γ lines with well balanced populations and depopulations of all levels. Our Munich Tandem Accelerator provides polarized deuteron beams with high precision and the Q3D spectrograph has a high resolution focal plane detector. Using the (d, p) reaction this allows the measurement of angular distributions and asymmetries for many levels and consequently unambiguous determination of spins, parities, and spectroscopic factors. We report these results for ^{24}Na.

II. EXPERIMENTAL DETAILS

A. The (d, p) reaction measurement

The reaction ^{23}Na$(d, p)^{24}$Na was measured with the Q3D spectrograph [29] at the tandem accelerator of the University

*Corresponding author. Email address: tomandl@ujf.cas.cz
†Deceased.

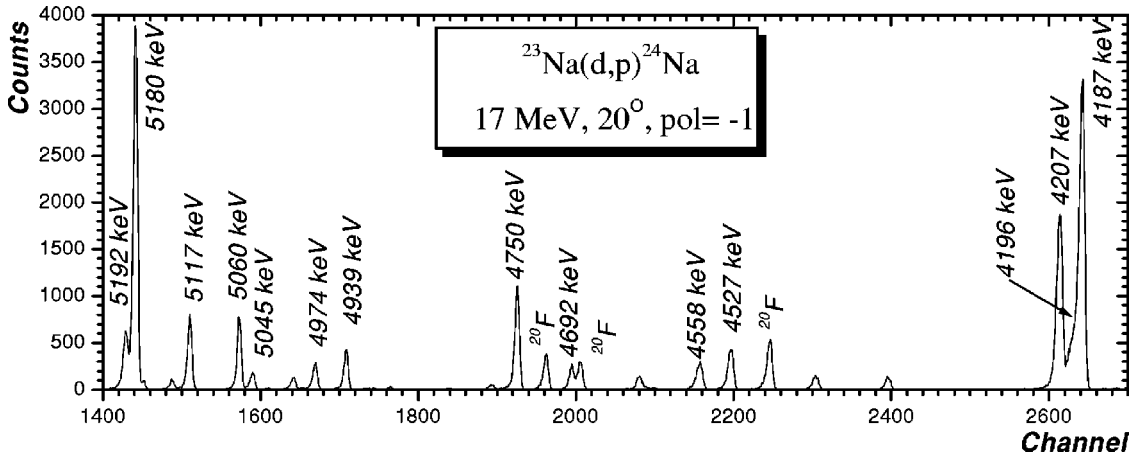

FIG. 1. A portion of the proton spectrum from the ^{23}Na$(d, p)^{24}$Na reaction with 17 MeV deuterons at $\Theta_{lab}=20°$. Differential cross sections at this angle are given in Table IV.

and Technical University of Munich. The total amount of 80 μg/cm^2 of NaF material (43.81 μg/cm^2 of ^{23}Na) on a 4.2 μg/cm^2 carbon backing was placed in the polarized beam of 17 MeV deuterons. Energies and intensities of protons were measured with the 1.7 m long focal plane detector [30]. A typical energy resolution [full width at half maximum (FWHM)] varied from 5 keV to 8 keV going from 12° to 50° of scattering angles. Altogether 30 overlapping proton spectra were taken for five scattering angles and two directions of the vector polarization of the deuterons. These overlapping spectra covered excitation energies up to ≈6.3 MeV. All spectra were normalized with respect to the beam current accumulated by a Faraday cup. Many fluorine lines in the spectra were easily recognized thanks to their position shifts at different angles. A representative spectrum taken at a laboratory scattering angle $\Theta_{lab}=20°$ is shown in Fig. 1.

Besides the angular distribution of the partial cross sections, also asymmetries were analyzed. The asymmetries were deduced from the equation

$$A_y = \frac{2}{3P_y}\frac{\sigma_+ - \sigma_-}{\sigma_+ + \sigma_-}, \qquad (1)$$

where σ_+ and σ_- are measured differential cross sections with respect to the polarization of the beam and where P_y is the vector polarization. In our experiment, the value of the vector polarization amounts to 0.6.

The energy calibration was performed with level energies from the (n, γ) reaction in the present work given in Table IV. Level energies averaged over all scattering angles are given in Table II. Maximal systematic errors of the level energies were estimated to be around 0.5 keV. Due to a lack of good calibration points above 6 MeV, additional uncertainties of 1 keV should be taken into account for levels above 6.1 MeV.

B. Analysis of angular distributions

The measured angular distributions of cross sections and vector analyzing powers were analyzed by means of the CHUCK3 code [31]. We studied three different sets of optical model potentials for the $d+^{23}$Na input channel. They were taken from the previous study of the ^{23}Na$(d, p)^{24}$Na reaction [32] at $E_d=7.8$ MeV and from compilations of optical model parameters [33,34] (see Table I). For the $p+^{24}$Na output channel two sets of potentials were considered. Calculations with various combinations of sets of optical model parameters were carried out for reactions leading to several low lying levels of the final ^{24}Na nucleus. After comparing calculated shapes of angular distributions of cross sections and vector analyzing powers with corresponding experimental

TABLE I. Parameters of the optical model for the ^{23}Na$(d, p)^{24}$Na reaction, $E_d=17$ MeV.

Pot	V [MeV]	r [fm]	a [fm]	W [MeV]	R_w [fm]	a_w [fm]	W_d [MeV]	r_d [fm]	a_d [fm]	V_so [MeV]	r_so [MeV]	a_so [fm]	r_c [fm]	Ref.
Input channel: $d+^{23}$Na														
A	58.0	1.544	0.452	11.5	1.544	0.452				10.0	1.25	0.65	1.3	[32]
B	89.8	1.203	0.698	39.3	0.903	0.539				11.21	1.0	0.585	1.3	[33]
C	87.5	1.17	0.738				12.28	1.325	0.728	7.82	1.07	0.66	1.3	[34]
Output channel: $p+^{23}$Na														
A	46.8	1.25	0.65				10.0	1.25	0.67	7.5	1.25	0.65	1.25	[33]
B	53.0	1.25	0.65				11.5	1.25	0.47	8	1.25	0.65	1.25	[32]

TABLE II. Spectroscopy of ^{24}Na via the ^{23}Na$(d, p)^{24}$Na reaction (E_d=17 MeV). Probable and possible levels are given in parentheses and curly brackets, respectively.

				$[(2J_f+1)/(2J_t+1)]S_{dp}$						
E_{lev}[a]	l=0	l=1		l=2		l=3		l=4		l=5
(keV)	$2s_{1/2}$	$2p_{1/2}$	$2p_{3/2}$	$1d_{3/2}$	$1d_{5/2}$	$1f_{5/2}$	$1f_{7/2}$	$1g_{7/2}$	$1g_{9/2}$	$1h_{11/2}$
0.0					0.60					
472.23 (12)					0.34					
563.08 (19)	0.056			0.05	0.18					
1341.25 (34)	0.21			0.076						
1346.37 (54)[b]	0.18				0.057					
1511.82 (16)					0.0020				0.025	
1846.33 (10)	0.094			0.14	0.13					
1885.27 (14)				0.08	0.12					
2512.33 (33)				0.06	0.06					
2563.16 (35)					0.069					
2904.06 (55)				0.029	0.029					
2977.70 (22)	0.11			0.24						
3216.57 (16)				0.003				0.029		
3371.55 (10)			0.20							
3413.05 (6)	0.11			0.09	0.14					
3589.31 (8)	0.020			0.018	0.026					
3628.58 (6)				0.29						
3656.10 (6)				0.12						
3681.13 (23)				0.005						
(3737.62 (22))				0.020	0.013			0.087		
3745.07 (13)			0.29							
3884.85 (32)										
3933.60 (13)					0.14					
3943.57 (8)				0.065	0.065					
3976.95 (29)			0.039							
4048.25 (20)			0.0013							
4142.59 (21)									0.010	
4187.30 (12)					0.44					
4196.42 (16)			0.015							
4207.03 (8)		0.044	0.096							
4441.75 (10)		0.013								
4526.87 (24)			0.004			0.098				
4559.07 (18)			0.002			0.056				
4621.12 (19)			0.0007			0.017				
4693.30 (15)			0.0014			0.025	0.010			
4750.78 (17)		0.011				0.11	0.11			
4889.31 (18)										0.063
4908.28 (16)								0.006	0.006	
4938.90 (13)						0.042	0.042			
4973.83 (12)			0.002			0.039				
5027.33 (49)								0.012		
5044.49 (17)		0.0031				0.018				
5059.95 (10)		0.032					0.028			
5117.34 (8)	0.26									
5180.55 (13)			0.025			0.15	0.23			
5192.51 (14)			0.014			0.017	0.017			

TABLE II. (*Continued.*)

				$[(2J_f+1)/(2J_t+1)]S_{dp}$						
E_{lev}[a]	$l=0$	$l=1$		$l=2$		$l=3$		$l=4$		$l=5$
(keV)	$2s_{1/2}$	$2p_{1/2}$	$2p_{3/2}$	$1d_{3/2}$	$1d_{5/2}$	$1f_{5/2}$	$1f_{7/2}$	$1g_{7/2}$	$1g_{9/2}$	$1h_{11/2}$
5245.38 (12)			0.012			0.016				
5308.10 (19)			0.0007			0.003				
5338.86 (10)		0.006				0.025	0.017			
{5397.61 (34)}										
5408.29 (24)	0.012									
5454.99 (21)							0.0061			
5478.88 (21)		0.002				0.025	0.017			
5571.57 (19)				0.005					0.041	
5629.27 (71)		0.0003				0.011				
5674.46 (27)	0.033									
5737.15 (16)			0.002				0.028			
5772.50 (42)		0.002				0.024				
(5789.41 (93))									0.016	
5808.44 (13)			0.001			0.008				
5850.65(16)			0.010			0.066	0.044			
5896.69 (9)									0.057	
5918.10 (13)	0.017				0.044					
6073.31 (21)				0.024				0.066		
(6088.20 (52))						0.021	0.014			
(6175.94 (52))			0.015				0.0016			
(6183.13 (65))							0.020			
(6199.11 (24))								0.013	0.026	
(6223.51 (4))										
6247.67 (13)			0.002			0.026				
6256.67 (15)			0.003			0.014	0.022			
6305.92 (53)					0.019			0.012		

[a]Only statistical error given.
[b]Unresolved doublet.

data, the combination of the parameter set *C* for the input channel and of the parameter set *B* for the output channel was chosen as the best one and was used for the calculations of all transfers to measured transitions in the final nucleus.

The spin of the target nucleus ^{23}Na is $J^{\pi}=3/2^{+}$. Due to this nonzero spin of the target nucleus the final angular distributions can result from mixing of up to four different (lj) transfers. We restrict our distorted-wave Born approximation (DWBA) analysis to two most significant l transfers and three (lj) transfers. Examples of levels fitted with the combination of (lj) transfers are given in Fig. 2. On the other hand, observed (lj) transfer will not provide a unique spin assignment, but only a restriction for a spin of a final level. More observed (lj) transfers can decrease a number of possible spins. We used the combination of different (lj) transfers for a spin assignment if other combinations could be clearly rejected.

The shape of the distribution of the differential cross section should determine the value of the transferred l. Usually, we have for the odd ^{23}Na target nucleus two possible transferred l, each with two values of j. Sometimes it is possible to determine the transferred j according to measured values of the vector analyzing power. With respect to very small dependence of the angular distribution of the cross section on the transferred j the contributions of transferred l and j were fitted separately. However, it should be noted that the division of the strength into G_{nlj} contributions has larger uncertainties than the contributions of l transfers. Moreover, these uncertainties significantly differ for various levels. Generally, it can be stated that these uncertainties are smaller for levels with the distribution of the differential cross section and of the vector analyzing power well reproduced or levels with one dominating l transfer. Values of deduced spectroscopic factors for different (l, j) transfers are given in Table II. These experimental G_{nlj} for the negative parity states were compared with the shell-model prediction published in Ref. [35]. The agreement between our experimental values and theoretical shell-model calculations is reasonable (see Fig. 3).

TABLE III. List of observed γ transitions with their absolute intensities per 100 neutron captures and placements.

E_γ (keV)[a]	I_γ[b]	Placement	E_γ (keV)[a]	I_γ[b]	Placement	E_γ (keV)[a]	I_γ[b]	Placement
91.01 *3*	46.0 *10*	563→472	1231.5 *4*	0.038 *5*	3745→2513	2130.8 *4*	0.038 *6*	3977→1846
373.11 *15*	0.015 *2*	3745→3372	1247.43 *7*	0.223 *7*	5809→4562	2139.4[c] *4*	0.034 *7*	5117→2978
472.23 *3*	92.2 *12*	472→0	1282.75 *3*	1.028 *15*	1846→563	2208.37 *3*	5.28 *4*	C→4751
499.41 *3*	2.72 *5*	1846→1347	1314.58 *17*	0.060 *6*	5060→3745	2220.0[d] *4*	0.17 *5*	5809→3589
501.46 *6*	0.58 *2*	1846→1345	1322.29 *3*	1.181 *12*	1886→563	2237.48 *12*	0.150 *7*	4751→2513
504.61 *5*	0.286 *10*	1846→1341	1337.74 *3*	0.646 *10*	4751→3413	2242.3 *5*	0.157 *17*	3589→1347
551.2 *3*	0.051 *12*	4207→3656	1344.55 *3*	4.07 *3*	1345→0	2247.83 *25*	0.082 *7*	3589→1341
552.72 *20*	0.104 *5*	unplaced	1373.74 *3*	1.54 *2*	1846→472	2266.7 *5*	0.063 *10*	C→4693
563.20 *3*	1.68 *2*	563→0	1379.2[e] *6*	0.034 *15*	4751→3372	2279.3 *4*	0.048 *10*	6257→3977
592.67 *15*	0.045 *3*	unplaced	1477.4 *5*	0.019 *5*	5455→3977	2283.0 *4*	0.087 *10*	3628→1345
605.46 *18*	0.035 *3*	3977→3372	1480.45 *5*	0.341 *7*	C→5479	2286.62 *19*	0.215 *12*	3628→1341
696.69 *19*	0.040 *3*	4442→3745	1486.14 *6*	0.228 *6*	3372→1886	2313.7 *7*	0.039 *10*	3656→1341
702.13 *16*	0.051 *4*	4751→4049	1504.83 *5*	0.469 *10*	C→5455	2334.9 *6*	0.022 *5*	3682→1347
708.20 *5*	0.22 *4*	C→6251	1526.1[f] *6*	0.017 *5*	4939→3413	2338.02 *20*	0.104 *10*	C→4621
711.97 *4*	0.842 *10*	C→6248	1559.25 *5*	0.295 *7*	2904→1345	2341.1 *6*	0.018 *2*	2904→563
773.85 *14*	0.11 *6*	4751→3977	1562.39 *4*	0.489 *10*	2904→1341	2350.0 *3*	0.073 *15*	4196→1846
778.23 *5*	1.154 *12*	1341→563	1567.18 *8*	0.101 *5*	3413→1846	2360.94 *3*	1.638 *17*	4207→1846
781.39 *5*	3.21 *3*	1345→563	1584.17 *16*	0.051 *5*	4562→2978	2397.32 *7*	1.19 *2*	C→4562
783.40 *22*	0.123 *10*	1347→563	1620.41 *4*	0.581 *10*	C→5339	2400.3 *3*	0.249 *15*	3745→1345
785.8[g] *3*	0.035 *6*	4442→3656	1631.04[h] *15*	0.172 *12*	2978→1347	2403.42 *15*	0.281 *12*	3745→1341
793.86 *4*	0.392 *7*	4207→3413	1633.10 *4*	1.154 *12*	2978→1345	2414.40 *3*	4.94 *4*	2978→563
813.0 *5*	0.012 *5*	4442→3628	1636.25 *3*	4.81 *4*	2978→1341	2431.9 *4*	0.080 *12*	2904→472
835.31 *3*	2.14 *2*	4207→3372	1715.2[d] *4*	0.021 *7*	4693→2978	2505.39 *3*	3.21 *3*	2978→472
852.36 *11*	0.066 *4*	4442→3589	1743.21 *17*	0.082 *7*	3589→1846	2513.5 *4*	0.085 *5*	2514→0
869.20 *3*	20.74 *17*	1341→472	1767.18 *24*	0.059 *5*	C→5192	2517.67 *3*	14.13 *12*	C→4442
874.37 *3*	14.59 *12*	1347→472	1770.3 *3*	0.062 *6*	3656→1886	2545.9[i] *5*	0.034 *6*	5060→2513
886.76 *6*	0.76 *2*	C→6073	1773.17 *8*	0.194 *7*	4751→2978	2555.8 *3*	0.069 *6*	4442→1886
992.6 *5*	0.014 *3*	4621→3628	1809.8 *4*	0.044 *6*	3656→1846	2588.73 *13*	0.242 *15*	3934→1345
999.7 *3*	0.022 *3*	3977→2978	1832.04 *11*	0.158 *6*	5809→3977	2592.10 *12*	0.375 *15*	3934→1341
1006.01 *3*	0.472 *7*	4751→3745	1842.17 *4*	0.460 *10*	C→5117	2595.46 *5*	0.956 *17*	4442→1846
1012.5 *5*	0.012 *3*	5455→4442	1847.11 *17*	0.091 *5*	4751→2904	2630.45 *5*	0.569 *12*	3977→1346
1018.3 *5*	0.013 *3*	2904→1886	1859.2 *3*	0.072 *6*	3745→1886	2657.8 *6*	0.029 *7*	6248→3589
1028.40 *17*	0.064 *5*	4442→3413	1885.42 *6*	0.721 *15*	1886→0	2702.0 *5*	0.031 *10*	4049→1347
1041.20 *5*	0.281 *7*	C→5918	1898.88[j] *3*	0.80[k] *10*	3745→1846	2715.78 *5*	0.576 *12*	4562→1846
1057.9 *3*	0.025 *5*	2904→1846	1899.73[j] *7*	0.80[k] *10*	C→5060	2752.23 *5*	11.5	C→4207
1092.22 *5*	0.319 *7*	2978→1886	1914.37 *4*	1.18 *17*	C→5045	2763.14 *11*	0.43 *3*	C→4196
1095.00 *8*	0.128 *5*	4751→3656	1928.22 *4*	0.937 *17*	4442→2513	2808.35 *3*	3.2 *3*	3372→563
1108.37 *4*	0.030 *4*	unplaced	1950.07 *3*	1.735 *15*	2513→563	2849.95 *9*	0.303 *10*	3413→563
1131.7[l] *3*	0.032 *5*	2978→1846	2019.86 *5*	0.663 *12*	C→4939	2860.25 *3*	3.58 *10*	4207→1346
1142.7[m] *7*	0.014 *7*	3656→2513	2025.04 *3*	6.28 *5*	3372→1347	2865.27[j] *3*	0.53[n] *7*	4751→1886
1150.00 *4*	0.983 *15*	C→5809	2027.13 *13*	0.76 *4*	3372→1345	2865.45[j] *2*	2.23[n] *10*	4207→1341
1172.1 *4*	0.028 *4*	2513→1341	2030.22 *3*	4.07 *4*	3372→1341	2875.4 *6*	0.019 *7*	6248→3372
1218.2 *5*	0.024 *4*	4196→2978	2048.27 *24*	0.102 *10*	4562→2513	2898.9 *6*	0.036 *7*	3372→472
1220.9 *5*	0.021 *4*	unplaced	2066.56 *9*	0.252 *12*	3413→1347	2903.70[j] *4*	0.121 *12*	2904→0
1225.0 *6*	0.016 *4*	5918→4693	2071.48 *3*	1.096 *17*	3413→1341	2904.78[j] *3*	1.07 *2*	4751→1846
1229.28 *5*	0.295 *7*	4207→2978	2087.48 *14*	0.133 *10*	3934→1846	2910.8 *4*	0.070 *10*	C→4049
2940.79 *5*	0.646 *12*	3413→472	3594.2 *5*	0.056 *7*	4939→1345	4553.5 *3*	0.085 *10*	5117→563
2977.8 *4*	0.121 *10*	2978→0	3597.4 *4*	0.070 *7*	4939→1341	4571.14[j] *5*	0.138 *15*	5918→1347

TABLE III. (*Continued.*)

E_γ (keV)[a]	I_γ[b]	Placement	E_γ (keV)[a]	I_γ[b]	Placement	E_γ (keV)[a]	I_γ[b]	Placement
2982.00 *3*	2.61 *4*	C→3977	3627.98 *21*	0.148 *10*	3628→0	4572.32[j] *4*	0.087 *10*	5045→472
3016.0 *3*	0.067 *6*	C→3943	3632.7[o] *3*	0.102 *10*	4196→563	4586.91 *18*	0.423 *10*	5060→472
3025.65[j] *8*	2.03[p] *10*	C→3934	3643.54 *3*	1.331 *2*	4207→563	4628.7 *5*	0.039 *7*	5192→563
3025.89[j] *5*	0.73[p] *7*	3589→563	3698.07 *13*	0.184 *7*	5045→1347	4644.7 *4*	0.058 *10*	5117→472
3088.9 *4*	0.090 *12*	unplaced	3703.30 *7*	0.404 *10*	5045→1341	4693.1 *8*	0.015 *5*	4693→0
3092.52[j] *6*	0.31 *2*	3656→563	3723.45 *22*	0.31 *2*	4196→472	4725.56[j] *6*	0.092 *10*	6073→1347
3094.80[j] *3*	0.54 *6*	4442→1347	3734.6 *5*	0.075 *15*	4207→472	4727.58[j] *7*	0.024 *7*	6073→1345
3096.83[j] *3*	3.51 *7*	4442→1345	3744.3 *9*	0.034 *12*	3745→0	4730.74[j] *6*	0.358 *15*	6073→1341
3099.93 *7*	2.64 *7*	4442→1341	3770.7 *6*	0.087 *10*	5117→1347	4775.23 *18*	0.167 *12*	5339→563
3116.89 *5*	0.905 *15*	3589→472	3866.5 *6*	0.024 *7*	unplaced	4890.87 *15*	0.305 *17*	5455→563
3168.3 *3*	0.039 *10*	6073→2904	3878.07 *3*	4.31 *7*	4442→563	4900.3 *3*	0.136 *12*	6248→1347
3174.2 *5*	0.036 *12*	5060→1886	3942.8 *5*	0.075 *12*	3943→0	4904.3 *4*	0.104 *12*	6251→1347
3181.54 *21*	0.242 *15*	3745→563	3969.05 *12*	0.416 *15*	4442→472	4908.6 *6*	0.036 *10*	6251→1341
3184.1 *6*	0.073 *15*	3656→472	3981.32 *4*	13.38 *12*	C→2978	4915.0 *5*	0.068 *10*	5479→563
3198.85 *13*	0.191 *10*	5045→1846	3997.44 *20*	0.300 *15*	5339→1341	4982.7 *7*	0.063 *15*	5455→472
3209.32 *5*	0.721 *15*	3682→472	4055.22 *11*	0.72 *3*	C→2904	5005.8 *7*	0.048 *15*	5479→472
3214.19 *4*	1.036 *15*	C→3745	4058.3 *6*	0.053 *12*	4621→563	5058.7 *7*	0.029 *10*	5060→0
3231.6 *6*	0.024 *5*	5117→1886	4089.27 *13*	0.43 *2*	4562→472	5073.38 *10*	0.419 *17*	C→1886
3270.81 *24*	0.104 *7*	5117→1846	4107.6 *7*	0.031 *10*	5455→1347	5112.85 *11*	0.53 *2*	C→1846
3277.38 *5*	0.704 *15*	C→3682	4131.7 *9*	0.024 *7*	5479→1347	5336.9 *7*	0.012 *5*	5809→472
3303.25 *9*	0.223 *7*	C→3656	4137.11 *24*	0.155 *15*	5479→1341	5445.33 *12*	0.160 *10*	5918→472
3330.93 *12*	0.235 *10*	C→3628	4187.35 *3*	1.52 *3*	4751→563	5599.85 *24*	0.121 *10*	6073→472
3343.30 *12*	0.256 *10*	6248→2904	4226.7 *7*	0.036 *12*	6073→1846	5612.12[j] *3*	0.148 *15*	C→1347
3369.87[j] *5*	1.55[p] *10*	C→3589	4278.8 *5*	0.019 *7*	4751→472	5614.15[j] *3*	0.41 *3*	C→1345
3370.12[j] *8*	1.16[p] *10*	3934→563	4361.7 *9*	0.018 *6*	6248→1886	5617.30[j] *2*	4.02 *10*	C→1341
3409.29 *7*	0.448 *12*	4751→1341	4376.05 *25*	0.106 *10*	4939→563	5683.8 *7*	0.012 *5*	6248→563
3413.81 *6*	0.813 *15*	3977→563	4404.4 *3*	0.046 *7*	6251→1846	5703.2 *3*	0.031 *7*	6176→472
3492.9 *3*	0.080 *7*	5339→1846	4445.64 *8*	0.494 *15*	C→2513	5774.41 *17*	0.235 *15*	6248→472
3504.78 *4*	1.32 *2*	3977→472	4462.39 *16*	0.140 *10*	5809→1347	5784.4 *5*	0.017 *7*	6257→472
3545.93 *4*	0.941 *15*	C→3413	4466.89 *11*	0.281 *12*	4939→472	6295.30 *6*	18.61 *12*	C→563
3576.7 *4*	0.078 *10*	4049→472	4481.38 *15*	0.177 *10*	5045→563	6486.16 *14*	0.41 *2*	C→472
3587.42 *4*	11.47 *10*	C→3372	4495.97 *8*	0.407 *15*	5060→563	6957.6 *9*	0.0027 *10*	C→0

[a]In our notation, 91.01 *3*≡91.01±0.03 etc.
[b]Intensity per 100 neutron captures. In our notation, 46.0 *10*≡46.0±1.0 etc.
[c]Can be also placed as a 6072→3933 transition.
[d]Obscured by the single-escape peak or full-energy peak from the 2223 keV γ ray in ^{2}H. I_γ from Grenoble data.
[e]Can be also placed as a 6072→4693 transition.
[f]Can be also placed as a 3371→1846 transition.
[g]Can be also placed as a 5478→4693 transition.
[h]Can be also placed as a 6072→4441 transition.
[i]Can be also placed as a 5918→3371 transition.
[j]Deduced for one member of a close doublet from level energies obtained by an overall least-square fit excluding this transition.
[k]Inferred from the intensity balance requirements for the 3744 and 5059 keV levels.
[l]Can be also placed as a 5338→4207 transition.
[m]Can be also placed as a 5338→4196 transition.
[n]Inferred from the intensity balance requirements simultaneously for the 1341 and 4750 keV.
[o]Can be also placed as a 5478→1846 transition.
[p]Inferred from the intensity balance requirements simultaneously for the 3589 and 3933 keV.

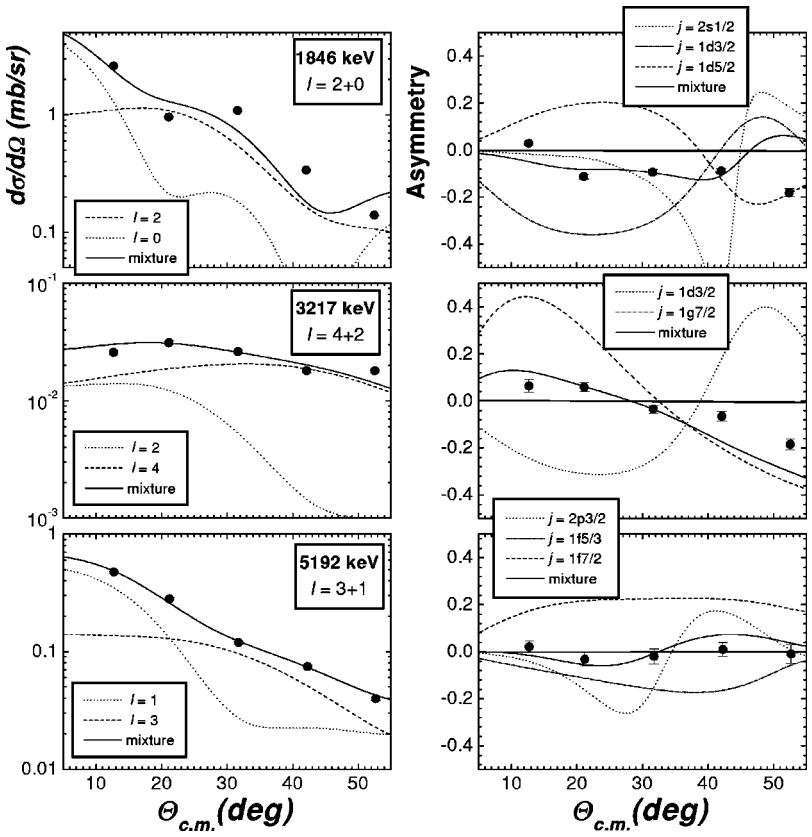

FIG. 2. Examples of the DWBA fit of the angular distribution of the differential cross section and the vector analyzing power.

C. The (n, γ) measurement

For the measurement of the ^{23}Na(n, γ) reaction the target was placed in the thermal column of the internal target facility at the 8-MW Los Alamos Omega West reactor. The target was irradiated with a neutron flux of $\sim 6 \times 10^{11}$ n/cm^2 s. This flux was approximately Maxwellian corresponding to a temperature of 350 K. Gamma ray spectra were measured with a 30 cm^3 coaxial intrinsic HPGe detector positioned inside a Na(Tl) annulus. More details about the facility and the data processing can be found in Refs. [4,6].

The primary calibration energies were those recommended by Wapstra [36]: 511.000 ± 0.002 keV for annihilation radiation; 2223.253 ± 0.004 keV for the γ ray from the ^{1}H(n, γ) reaction and 4945.303 ± 0.030 keV for the ground state transition in the ^{12}C(n, γ) reaction. Absolute intensities of γ lines were derived from the assumption that the population of the ground state amounts to 100% after neutron capture. The list of all observed γ lines together with their absolute intensities per 100 neutron captures and their placements is given in Table III.

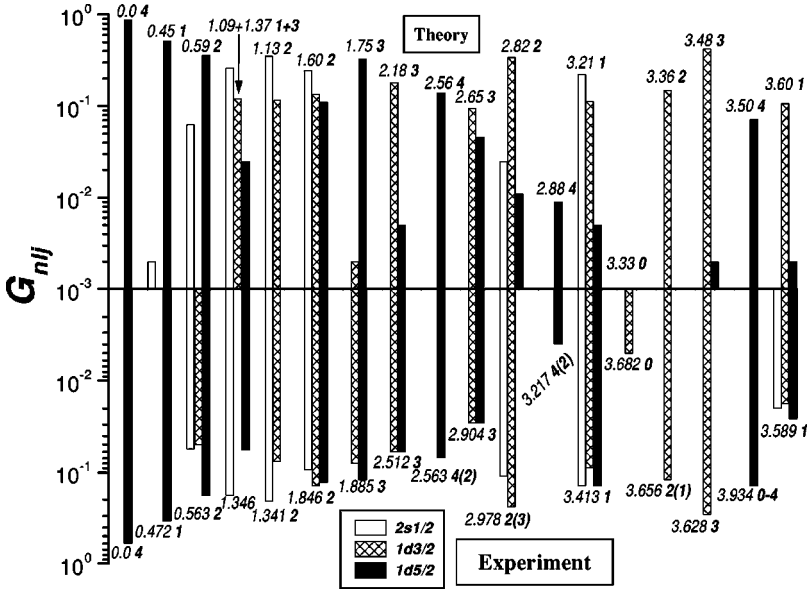

FIG. 3. Comparison of the experimental (lower plot) and calculated (upper plot) $G_{nlj} = [(2J_f+1)/(2J_i+1)]S_{dp}$ transfer strength. Theoretical values are shell-model calculation from Ref. [35]. The levels are labeled by their excitation energies (italic) and spins (bold). Note that our experimental data prefer $1d3/2$ transfer for the 3217 keV level. However $1d5/2$ transfer cannot be fully disregarded. Thus, we accepted for this level the previous spin assignment from Nuclear Data Sheets (NDS), $4^+(2^+)$, and used $1d5/2$ transfer in the comparison.

TABLE IV. Level scheme of ^{24}Na in tabular form. Tentative levels in our experments are set in italic typeface.

	(n, γ)		(d, p)	$(d\sigma/d\Omega)^{exp.}$	This work	NDS [7]		Adopted
E (level) (keV)	I_γ (in) per 100 n	I_γ (out) per 100 n	E (level) (keV)	(mb/sr) at 20°	J^π	E (level)	J^π	J^π
0.0	100 (1)		0.0	1.56	1^+-4^+	0	4^+	4^+
472.222 (18)	94.7 (10)	92.9 (12)	472.23 (12)	1.15	1^+-4^+	472.207 (9)	1^+	1^+
563.215 (18)	47.5 (3)	49.1 (10)	563.08 (19)	0.87	$1^+, 2^+$	563.200 (12)	2^+	2^+
1341.435 (19)	22.5 (2)	21.9 (2)	1341.25 (34)	0.79	$1^+, 2^+$	1341.43 (2)	2^+	2^+
1344.590 (19)	7.38 (9)	7.29 (4)			$2^+, 3, 4^+$	1344.65 (2)	$3^{(+)}$	$3^{(+)}$
1346.616 (21)	15.4 (2)	14.7 (1)	1346.37 (54)[a]	0.46		1346.63 (2)	1^+	1^+
			1511.82 (16)	0.021	$3^+, 4^+(5^+, 6^+)$	1512.4 (4)	$5^+(3^+)$	$5^+(3^+)$
1846.016 (21)	6.56 (11)	6.16 (6)	1846.33 (10)	1.06	$1^+, 2^+$	1846.01 (3)	2^+	2^+
1885.530 (24)	1.79 (7)	1.90 (2)	1885.27 (14)	0.81	$2^+, 3^+$	1885.51 (5)	3^+	3^+
2513.36 (3)	1.77(20)	1.85 (2)	2512.33 (33)	0.56	$2^+, 3^+$	2513.51 (5)	3^+	3^+
			2563.16 (35)	0.30	1^+-4^+	2562.8 (3)	$4^+(2^+)$	$4^+(2^+)$
2903.89 (3)	1.11(3)	1.04 (2)	2904.06 (55)	0.089[b]	$2^+, 3^+$	2903.94 (5)	3^+	3^+
2977.749 (21)	14.04 (2)	14.78 (7)	2977.70 (22)	1.44	$1^+, 2^+$	2977.83 (4)	$2^+(3^+)$	2^+
			3216.57 (16)	0.035	$2^+, 3^+(4^+)$	3216.7 (2)	$4^+(2^+)$	$4^+(2^+)$
3371.744 (22)	13.7 (1)	14.6 (3)	3371.55 (10)	2.32	2^-	3371.84 (4)	2^-	2^-
3413.219 (23)	2.06 (2)	2.40 (21)	3413.05 (6)	1.11	$1^+, 2^+$	3413.25 (5)	1^+	1^+
3589.32 (3)	1.82 (11)	1.96 (7)	3589.31 (8)	0.21	$1^+, 2^+$	3589.26 (10)	1^+	1^+
3628.24 (9)	0.26 (1)	0.45 (2)	3628.58 (6)	1.47	$2^+, 3^+$	3628.25 (11)	3^+	3^+
3655.95 (4)	0.44 (1)	0.54 (3)	3656.10 (6)	0.59	1^+-3^+	3655.97 (9)	$2(1)^+$	$2(1)^+$
3681.80 (4)	0.71 (2)	0.74 (2)	3681.13 (23)	0.022	0^+-3^+	3681.79 (8)	0^+	0^+
			3737.62 (22)[c]	0.23	2^+-4^+			2^+-4^+
3744.97 (3)	1.61 (2)	1.73 (10)	3745.07 (13)	2.61	3^-	3745.09 (7)	3^-	3^-
			3884.85 (32)	0.012[d]		3896 (6)	$(1, 2, 3)^-$	
3933.59 (5)	2.0 (1)	1.9 (1)	3933.60 (13)	0.56	1–4	3935.7 (4)	0^+-4^+	1–4
3943.2 (3)	0.07 (1)	0.08 (1)	3943.57 (8)	0.49	$2^+, 3^+$	3943.39 (17)	2^+-6^+	$2^+, 3^+$
3977.25 (3)	2.95 (7)	2.80 (3)	3976.95 (29)	0.14	$1^-, 2^-$	3977.32 (7)	$(1^-, 2^+)$	$1^-(2^-)$
4048.84 (14)	0.12 (1)	0.11 (1)	4048.25 (20)	0.012	0^--2^-	4048.49 (16)	0^-	0^-
			4142.59 (21)	0.011	3^+-6^+	4145.0 (9)	$4^-(5^-)$	3^+-6^+
			4187.30 (12)	2.29	1^+-4^+	4186.8 (3)	2^+	2^+
4196.11 (9)	0.43 (3)	0.51 (3)	4196.42 (16)	0.25	$1^-, 2^-$	4196.3 (2)	$(1, 2)^-$	$1^-, 2^-$
4207.066 (22)	11.5 (5)	11.7 (2)	4207.03 (8)	1.26	$1^-, 2^-$	4207.19 (4)	2^+	$1^-, 2^-$
						4220 (3)		
4441.632 (21)	14.2 (1)	13.6 (2)	4441.75 (10)	0.12	2^-	4441.54 (11)	2^-	2^-
						4459 (8)		
			4526.87 (24)	0.25	1^--3^-	4526 (8)	3^-	3^-
			4559.07 (18)[c]	0.18	1^--3^-			1^--3^-
4561.94 (4)	1.42 (2)	1.16 (10)			$1^+, 2, 3^+$	4562.06 (6)	1^-	$1^+, 2, 3^+$
4621.30 (18)	0.10 (1)	0.07 (1)	4621.12 (19)	0.081	2^-	4621.5 (2)		2^-
4693.0 (3)	0.08 (1)	0.04 (1)	4693.30 (15)	0.14	3^-	4692.2 (4)		3^-
4750.984 (21)	5.29 (4)	5.47 (10)	4750.78 (17)	0.70	2^-	4750.94 (10)	2^-	2^-
						4772 (7)		
			4889.31 (18)	0.012	3^--7^-	4891.35 (16)	$(3^+, 4^-, 5^+)$	(4^-)
			4908.28 (16)	0.007	2^+-6^+			2^+-6^+
4939.50 (5)	0.66 (1)	0.53 (2)	4938.90 (13)	0.24	2^-	4939.40 (11)	$(1, 3)^-$	2^-
			4973.83 (12)	0.15	1^--3^-	4980 (7)		1^--3^-
			5027.33 (49)	0.007	$\geqslant 2$	5030 (2)		$\geqslant 2$

TABLE IV. (*Continued.*)

(n, γ)			(d, p)	$(d\sigma/d\Omega)^{exp.}$	This work	NDS [7]		Adopted
E (level) (keV)	I_γ (in) per 100 n	I_γ (out) per 100 n	E (level) (keV)	(mb/sr) at 20°	J^π	E (level)	J^π	J^π
5045.01 (3)	1.18 (17)	1.04 (2)	5044.49 (17)	0.11	$1^-, 2^-$	5044.90 (11)	$(1, 2, 3)^-$	$1^-, 2^-$
5059.63 (5)	0.80 (10)	0.99 (3)	5059.95 (10)	0.46	$2^-(2^+, 3^+)$	5059.72 (6)	2^-	2^-
5117.22 (3)	0.46 (1)	0.39 (2)	5117.34 (8)	0.44	$1^+, 2^+$	5117.41 (16)	1^-	$1^+, 2^+$
						5160 (8)		
			5180.55 (13)	2.26	$1^- - 3^-$			$1^- - 3^-$
5192.23 (22)	0.06 (1)	0.04 (1)	5192.51 (14)	0.31	$1^- - 3^-$	5192.44 (16)	3^-	3^-
			5245.38 (12)	0.19	$1^- - 3^-$	5250 (2)	3^-	3^-
			5308.10 (19)[c]	0.009[b]	$1^- - 3^-$			$1^- - 3^-$
5338.99 (4)	0.58 (1)	0.55 (2)	5338.86 (10)	0.19[b]	$1^- - 3^-$	5339.06 (8)	2^-	2^-
			5397.61 (34)	0.037[e]		5397.19 (11)	$(1, 3)^-$	$(1, 3)^-$
			5408.29 (24)[c]	0.033	$1^+, 2^+$			$1^+, 2^+$
						5432 (8)	+	+
5454.57 (5)	0.47 (1)	0.43 (3)	5454.99 (21)	0.008[d]	$1, 2(3^+)$			$1, 2(3^+)$
5478.94 (5)	0.34 (1)	0.30 (2)	5478.88 (21)	0.14[b]	$1^-, 2^-$	5478.96 (9)	1^-	1^-
			5571.57 (19)[c]	0.093	$2^+ - 4^+$	5585 (8)	−	$2^+ - 4^+$
			5629.27 (71)	0.031		5628.4 (15)	2^-	2^-
			5674.46 (27)	0.042	$1^+, 2^+$	5660 (20)		$1^+, 2^+$
			5737.15 (16)	0.12	$1^- - 3^-$	5720 (20)		$1^- - 3^-$
			5772.50 (42)	0.11	$1^- - 3^-$	5774 (5)		$1^- - 3^-$
			5789.41 (93)[c]	0.030[b]	$3^+ - 6^+$			$3^+ - 6^+$
5809.41 (4)	0.98 (2)	0.70 (7)	5808.44 (13)	0.038	$1^-, 2^-$	5809.66 (12)		$1^-, 2^-$
			5850.65 (16)[c]	0.67	$1^- - 3^-$			$1^- - 3^-$
						5862.9 (2)		
			5896.69 (9)[c]	0.092	$3^+ - 6^+$			$3^+ - 6^+$
5918.22 (5)	0.28 (1)	0.31 (2)	5918.10 (13)	0.14[b]	$2^+(1^+)$	5918.46 (12)		$2^+(1^+)$
						5953.16 (10)		
						5966.2 (10)		
6072.67 (3)	0.76 (2)	0.67 (3)	6073.31 (21)	0.21	$2^+(3^+)$	6072.83 (13)	1^+	$2^+(3^+)$
			6088.20 (52)[c]	0.10[b]	$(1^- - 5^-)$			$(1^- - 5^-)$
6176.15 (30)[c]		0.03 (1)	*6175.94 (52)*[c]	0.039[b]	$(1^-, 2^-)$			$(1^-, 2^-)$
			6183.13 (65)[c]	0.092	$(1^- - 5^-)$			$(1^- - 5^-)$
			6199.11 (24)[c]	0.11	$(3^+ - 6^+)$			$(3^+ - 6^+)$
			6223.5 (6)	0.014[f]				
6247.46 (4)	0.84 (1)	0.71 (15)	6247.67 (13)	0.089	2^-	6247.62 (12)		2^-
6251.22 (5)[c]	0.22 (4)	0.19 (2)			$0^+, 1, 2, 3^+$			0^+,1,2, 3^+
6256.94 (31)[c]		0.07 (1)	6256.67 (15)[c]	0.15	$1^-, 2^-$			$1^-, 2^-$
			6305.92 (53)[c]	0.19	$2^+ - 4^+$			$2^+ - 4^+$
			1					
6959.444 (19)[g]	100.6 (6)							$1^+ + 2^+$

[a]Unresolved doublet.
[b]Value of partial cross section at 30°.
[c]New levels.
[d]Value of partial cross section at 40°.
[e]Value of partial cross section at 12°.
[f]Value of partial cross section at 50°.
[g]Capturing state.

TABLE V. Branching ratios for levels in ^{24}Na.

E_i (keV)	J_i^π	E_f (keV)	J_f^π	E_γ (keV)	Branching	E_i (keV)	J_i^π	E_f (keV)	J_f^π	E_γ (keV)	Branching
472	1^+	0	4^+	472.23	100			1347	1^+	2242.3	8.1
563	2^+	0	4^+	563.20	3.4			1846	2^+	1743.21	4.2
		472	1^+	91.01	96.6	3628	3^+	0	4^+	3627.98	32.8
1341	2^+	472	1^+	869.20	94.7			1341	2^+	2286.62	47.8
		563	2^+	778.23	5.3			1345	3^+	2283.0	19.4
1345	3^+	0	4^+	1344.55	55.9	3656	$2^+(1^+)$	472	1^+	3184.1	13.4
		563	2^+	781.39	44.1			563	2^+	3092.52	57.2
1347	1^+	472	1^+	874.37	99.2			1341	2^+	2313.7	7.2
		563	2^+	783.40	0.8			1846	2^+	1809.8	8.1
1846	2^+	472	1^+	1373.74	25.0			1886	3^+	1770.3	11.4
		563	2^+	1282.75	16.7			2513	3^+	1142.7	$\leqslant$2.7
		1341	2^+	504.61	4.7	3682	0^+	472	1^+	3209.32	97.1
		1345	3^+	501.46	9.4			1347	1^+	2334.9	2.9
		1347	1^+	499.41	44.2	3745	3^-	0	4^+	3744.3	2.0
1886	3^+	0	4^+	1885.42	37.9			563	2^+	3181.54	14.0
		563	2^+	1322.29	62.1			1341	2^+	2403.42	16.2
2513	3^+	0	4^+	2513.5	4.6			1345	3^+	2400.3	14.4
		563	2^+	1950.07	93.9			1846	2^+	1898.88	46.2
		1341	2^+	1172.1	1.5			1886	3^+	1859.2	4.1
2903	3^+	0	4^+	2903.70	11.6			2513	3^+	1231.5	2.2
		472	1^+	2431.9	7.7			3372	2^-	373.11	0.9
		563	2^+	2341.1	1.7	3934	1–4	563	2^+	3370.12	60.7
		1341	2^+	1562.39	46.9			1341	2^+	2592.10	19.6
		1345	3^+	1559.25	28.4			1345	3^+	2588.73	12.7
		1847	2^+	1057.3	2.4			1846	2^+	2087.48	7.0
		1886	3^+	1018.3	1.3	3943	$2^+,3^+$	0	4^+	3942.8	100
2978	2^+	0	4^+	2977.8	0.8	3977	$1^-(2^-)$	472	1^+	3504.78	47.2
		472	1^+	2505.39	21.7			563	2^+	3413.81	29.1
		563	2^+	2414.40	33.5			1347	1^+	2630.45	20.3
		1341	2^+	1636.25	32.6			1846	2^+	2130.8	1.4
		1345	3^+	1633.10	7.8			2978	2^+	999.7	0.8
		1347	1^+	1631.04	$\leqslant$1.2			3372	2^-	605.46	1.2
		1846	2^+	1131.7	$\leqslant$0.2	4049	0^-	472	1^+	3576.7	68.3
		1886	3^+	1092.22	2.2			1347	1^+	2702.0	31.7
3372	2^-	472	1^+	2898.9	0.3	4196	$1^-,2^-$	472	1^+	3723.45	61.3
		563	2^+	2808.35	21.9			563	2^+	3632.7	$\leqslant$19.8
		1341	2^+	2030.22	27.9			1846	2^+	2350.0	14.2
		1345	3^+	2027.13	5.2			2978	2^+	1218.2	4.7
		1347	1^+	2025.04	43.1	4207	$1^-,2^-$	472	1^+	3734.6	0.6
		1886	3^+	1486.14	1.6			563	2^+	3643.54	11.4
3413	1^+	472	1^+	2940.79	27.0			1341	2^+	2865.45	19.0
		563	2^+	2849.95	12.6			1347	1^+	2860.25	30.5
		1341	2^+	2071.69	45.7			1846	2^+	2360.94	14.0
		1347	1^+	2066.56	10.5			2978	2^+	1229.28	2.5
		1846	2^+	1567.18	4.2			3372	2^-	835.31	18.3
3589	1^+	472	1^+	3116.89	46.3			3413	1^+	793.86	3.3
		563	2^+	3025.89	37.2			3656	$2^+(1^+)$	551.2	0.4

TABLE V. (*Continued*.)

E_i (keV)	J_i^π	E_f (keV)	J_f^π	E_γ (keV)	Branching	E_i (keV)	J_i^π	E_f (keV)	J_f^π	E_γ (keV)	Branching
		1341	2^+	2247.83	4.2	4442	2^-	472	1^+	3969.05	3.1
		563	2^+	3878.07	31.7			2513	3^+	2545.9	4.7
		1341	2^+	3099.93	19.4			3745	3^-	1314.58	8.3
		1345	3^+	3096.83	25.8	5117	$1^+,2^+$	472	1^+	4644.7	14.8
		1347	1^+	3094.80	4.0			563	2^+	4553.5	21.6
		1846	2^+	2595.46	7.0			1347	1^+	3770.7	22.2
		1886	3^+	2555.8	0.5			1846	2^+	3270.81	26.5
		2513	3^+	1928.22	6.9			1886	3^+	3231.6	6.2
		3413	1^+	1028.40	0.5			2978	2^+	2139.4	$\leqslant$8.6
		3589	1^+	852.36	0.5	5192	3^-	563	2^+	4628.7	100
		3628	3^+	813.0	0.09	5339	2^-	563	2^+	4775.23	30.5
		3656	$2^+(1^+)$	785.8	$\leqslant$0.3			1341	2^+	3997.44	54.9
		3745	3^-	696.69	0.3			1846	2^+	3492.9	14.6
4562	$1^+,2,3^+$	472	1^+	4089.27	36.9	5455	$1,2(3^+)$	472	1^+	4982.7	14.6
		1846	2^+	2715.78	49.9			563	2^+	4890.87	70.9
		2513	3^+	2048.27	8.8			1347	1^+	4107.6	7.3
		2978	2^+	1584.17	4.4			3977	$1^-(2^-)$	1477.4	4.4
4621	2^-	563	2^+	4058.3	79.1			4442	2^-	1012.5	2.7
		3628	3^+	992.6	20.9	5479	1^-	472	1^+	5005.8	16.4
4693	3^-	0	4^+	4693.1	0.4			563	2^+	4915.0	23.0
		2978	2^+	1715.2	0.6			1341	2^+	4137.11	52.4
4751	2^-	472	1^+	4278.8	0.4			1347	1^+	4131.7	8.2
		563	2^+	4187.35	27.9	5809	$1^-,2^-$	472	1^+	5336.9	1.7
		1341	2^+	3409.29	8.2			1347	1^+	4462.39	20.0
		1846	2^+	2904.78	19.6			3589	1^+	2220.0	4.1
		1886	3^+	2865.27	9.7			3977	$1^-(2^-)$	1832.04	22.5
		2513	3^+	2237.48	2.7			4562	$1^+,2,3^+$	1247.43	31.7
		2904	3^+	1847.11	1.7	5918	$2^+(1^+)$	472	1^+	5445.33	50.9
		2978	2^+	1773.17	3.5			1347	1^+	4571.14	43.9
		3372	2^-	1379.2	$\leqslant$0.6			4693	3^-	1225.0	5.2
		3413	1^+	1337.74	11.8	6073	$2^+(3^+)$	472	1^+	5599.85	18.1
		3656	$2^+(1^+)$	1095.00	2.3			1341	2^+	4730.74	53.4
		3745	3^-	1006.01	8.6			1346	3^+	4727.58	3.6
		3977	$1^-(2^-)$	773.85	1.9			1347	1^+	4725.56	13.7
		4049	0^-	702.13	0.9			1846	2^+	4226.7	5.4
4939	2^-	472	1^+	4466.89	53.0			2904	3^+	3168.3	5.8
		563	2^+	4376.05	20.1	6176	$(1^-, 2^-)$	472	1^+	5703.2	100
		1341	2^+	3597.4	13.2	6248	2^-	472	1^+	5774.41	33.3
		1345	3^+	3594.2	10.5			563	2^+	5638.8	1.7
		3413	1^+	1526.1	$\leqslant$3.2			1347	1^+	4900.3	19.2
5045	$1^-, 2^-$	472	1^+	4572.32	8.4			1886	3^+	4361.7	2.5
		563	2^+	4481.38	16.9			2904	3^+	3343.30	36.4
		1341	2^+	3703.30	38.7			3372	2^-	2875.4	2.7
		1347	1^+	3698.07	17.6			3589	1^+	2657.8	4.1

TABLE V. (*Continued.*)

E_i (keV)	J_i^π	E_f (keV)	J_f^π	E_γ (keV)	Branching	E_i (keV)	J_i^π	E_f (keV)	J_f^π	E_γ (keV)	Branching
		1846	2^+	3198.85	18.3	6251	0^+,1,2, 3^+	1341	2^+	4908.6	19.7
5060	2^-	0	4^+	5058.7	4.0			1347	1^+	4904.3	56.6
		472	1^+	4586.91	21.7			1846	2^+	4404.4	23.7
		563	2^+	4495.97	56.2	6257	1^-,2^-	472	1^+	5784.4	25.9
		1886	3^+	3174.2	5.0			3977	$1^-(2^-)$	2279.3	74.1
6959	$1^+ + 2^+$	0	4^+	6957.6	0.0027						
		472	1^+	6486.16	1.69						
		563	2^+	6395.30	18.5						
		1341	2^+	5617.30	4.0						
		1345	3^+	5614.15	0.41						
		1347	1^+	5612.12	0.15						
		1846	2^+	5112.85	0.53						
		1886	3^+	5073.38	0.42						
		2513	3^+	4445.64	0.49						
		2904	3^+	4055.22	0.71						
		2978	2^+	3981.32	13.3						
		3372	2^-	3587.42	11.4						
		3413	1^+	3545.93	0.94						
		3589	1^+	3369.87	1.5						
		3628	3^+	3330.93	0.23						
		3656	$2^+(1^+)$	3303.25	0.22						
		3682	0^+	3277.38	0.70						
		3745	3^-	3214.19	1.0						
		3934	1–4	3025.65	2.0						
		3943	2^+, 3^+	3016.0	0.067						
		3977	$1^-(2^-)$	2982.00	2.6						
		4049	0^-	2910.8	0.070						
		4196	1^-, 2^-	2763.14	0.43						
		4207	1^-, 2^-	2752.23	11.4						
		4442	2^-	2517.67	14.1						
		4562	1^+,2, 3^+	2397.32	1.2						
		4621	2^-	2338.02	0.10						
		4693	3^-	2266.7	0.063						
		4751	2^-	2208.37	5.3						
		4939	2^-	2019.86	0.66						
		5045	1^-, 2^-	1914.37	1.2						
		5060	2^-	1899.73	0.8						
		5117	1^+, 2^+	1842.17	0.46						
		5192	3^-	1767.18	0.059						
		5339	2^-	1620.41	0.58						
		5455	1, $2(3^+)$	1504.83	0.47						

TABLE V. (*Continued.*)

E_i (keV)	J_i^π	E_f (keV)	J_f^π	E_γ (keV)	Branching	E_i (keV)	J_i^π	E_f (keV)	J_f^π	E_γ (keV)	Branching
		5479	1^-	1480.45	0.34						
		5809	1^-, 2^-	1150.00	0.98						
		5918	$2^+(1^+)$	1041.20	0.28						
		6073	$2^+(3^+)$	886.76	0.76						
		6248	2^-	711.97	0.84						
		6251	0^+,1,2, 3^+	708.20	0.23						

From the γ transitions placed in the level scheme we determined the neutron separation energy to be 6959.44 ± 0.05 keV. This precise value is in very good agreement with the result of Greenwood and Chrien [37], 6959.426 ± 0.076 keV as well as with value given in the Brookhaven National Laboratory compilation [38], 6959.40 ± 0.12 keV. The uncertainty of our deduced value includes the uncertainty in the primary calibration energies.

III. DISCUSSIONS OF LEVEL SCHEME AND ITS COMPLETENESS

One of the main goals of the present work is the construction of an essentially complete level scheme of ^{24}Na in the spin range up to ~ 6 and the energy range up to the neutron separation energy. Combining the (d, p) and (n, γ) data totally 75 levels were observed in this work in the range from 0 to 6.3 MeV. The list of these levels is given in Table IV. Fifteen levels from this list are reported for the first time. Most of them were observed in the (d, p) measurements at least at two angles (in four spectra). The establishment of the new level at 6251 keV is based on three depopulating and one populating transitions. The adopted spin-parity assignments in Table IV are made using results from both present and previous works. The decay scheme of levels follows from the (n, γ) measurement and is given in Table V.

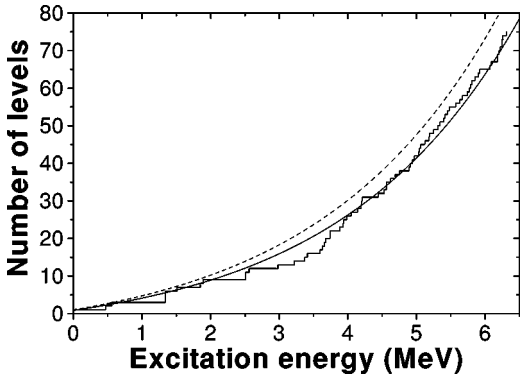

FIG. 4. The cumulative number of levels as a function of excitation energy. The steplike graph is the number of levels from this work. The smooth curves are predictions of the constant temperature Fermi gas model. The dashed line represents the total number of levels. The solid line shows model estimation for spin range from 0 to 6. The parameters for the constant temperature Fermi gas model are taken from Ref. [40].

The very high sensitivity in our (n, γ) and (d, p) measurements together with the good energy resolution in the (d, p) spectra allows us to establish a very firm correspondence between (n, γ) levels and those from transfer reaction measurements. Despite these high sensitivity measurements in this work, we have obtained no evidence for some levels previously reported and listed in the last ENSDF compilation [7]. These levels deserve special attention. Some of these together with some other levels are discussed below in detail.

The 3896±6 keV level. This level was observed only in the ^{26}Mg$(\vec{d}, \alpha)$ measurement [24]. In our work no evidence for any level with such energy was found. However, we established a new level at 3884.85 ± 0.32 keV. Note that a similar level was reported in the recent work done by Vernotte *et al.*, at 3884 keV. With respect to the large energy uncertainty in the ^{26}Mg$(\vec{d}, \alpha)$ experiment it is not possible to decide if there is a doublet or if we refer to the same level.

The 3935.7±0.4 keV and 4145.0±0.9 keV levels. In both our experiments we determined the energy of the first level to be 3933.6 keV. Our spin-parity assignment for this level is not in contradiction with that given in ENDSF compilation [7]. Thus most probably, these two different energy values refer to the same level. A similar case could be level 4145.0 keV which we found at the energy of 4142.6 ± 0.5 keV in the (d, p) experiment. Nevertheless, our parity assignment for this level disagrees with that from the previous works.

The doublet of levels at 4559.1±0.5 keV and 4561.94±0.04 keV. Almost 3 keV energy difference and different parity assignment lead us to establish this doublet of levels.

The 5397.19±0.11 keV and 5408.3±0.5 keV levels. In our work we observed peaks corresponding the 5397 keV level only in the (d, p) measurements and only at 12°. Thus, we cannot confirm the existence of this level. Close to this probable level we find the new level 5408.3 ± 0.2 keV. Note that Vernotte *et al.* [1] reported a level at 5402 keV. With respect to the energy resolution in their measurement, this proposed level could be a doublet of the previously seen level at 5397 keV and our newly proposed level at 5408 keV.

The 5846 keV and 5862.9±0.2 keV levels. Close to the

TABLE VI. Calculation of direct capture contribution for $E1$ transitions.

E_{lev} (keV)	E_γ (keV)	J^π	$S_{1/2}$	$S_{3/2}$	σ^{DC} (mb)	σ^{exp} (mb)	$\langle\sigma^{CN}\rangle$ (mb)
3371	3588	2^-		0.40	**19.8**	61	33
3745	3214	3^-		0.41	**0.73**	5.5	0.23
3977	2982	1^-		0.23	**4.9**	13.8	19
4048	2911	0^-		0.072	0.19	0.37	17
4196	2763	if 1^-		0.14	1.7	2.3	15
4196	2763	if 2^-		0.11	**1.1**	2.3	15
4207	2752	if 1^-	0.24	0.36	**18.4**	61	15
4207	2752	if 1^-	−0.24	0.36	5.6	61	15
4207	2752	if 2^-	0.24	0.36	18.3	61	15
4207	2752	if 2^-	−0.24	0.36	1.1	61	15
4441	2518	2^-	0.10		0.80	69	11
4526	2433	3^-		0.076	0.04		0.10
4559	2400	1^-		0.052	0.19		9.8
4621	2338	2^-		0.024	0.04	0.55	9.0
4693	2267	3^-		0.028	0.005	0.33	0.08
4750	2208	2^-	0.094		0.58	28	7.6
4974	1986	if 1^-		0.052	0.15		5.5
5044	1914	if 1^-	0.064		0.05	6.3	4.9
5044	1914	if 2^-	0.050		0.14	6.3	4.9
5059	1900	2^-	0.16		**1.4**	4.2	4.8
5180	1779	if 1^-		0.18	1.6		4.0
5180	1779	if 2^-		0.14	0.98		4.0
5180	1779	if 3^-		0.12	0.11		0.04
5192	1767	3^-		0.089	0.06	0.31	0.04
5245	1714	3^-		0.083	0.05		0.04
5338	1620	2^-	0.069		0.21	3.1	3.0
5478	1480	1^-	0.052		0.03	1.8	2.3
5808	1150	if 1^-		0.036	0.04	5.2	1.1
6176	784	if 1^-		0.141	0.35		0.34
6247	712	2^-	0.040		0.03	4.5	0.25

5846 keV level in $(d, {}^3\mathrm{He})$ [1] (which corresponds to our 5850.7 keV level) Vernotte *et al.* observed a level at 5863 keV, which could confirm the previously reported level 5862.9±0.2 keV [7]. However, we find no evidence in our work for this level.

The 5953.16±0.10 and 5966.2±1.0 keV levels. Neither of these levels was confirmed in our work. Nevertheless, our small angle (d, p) spectra in this energy region suffer from broad background lines from oxygen and carbon. Moreover, the 5966 keV level is considered to be the first $T=2$ state in ^{24}Na. Therefore, only multistep population of this level will be possible in the (d, p) reaction.

The 4220±3 keV, 4459±8 keV, 4772±7, 5160±8 keV, and 5432±8 keV levels. There is no explanation why we could not see these levels. Thus, we consider these levels at least as questionable.

To answer the important question of the completeness of our ^{24}Na level scheme we compared the number of levels from our work with the prediction of the constant temperature Fermi gas model [39]. With respect to spin sensitivity of reactions used in this work, we have estimated that we should be able to observe levels in the spin range from 0 to 6. For this spin range this model gives the cumulative number of levels up to the excitation energy E with the formula

$$N(E) = \sum_{J=0}^{6} f(J)\exp[(E - E_0)/T] + c. \tag{2}$$

The spin distribution is given by

$$f(J) = \exp(-J^2/2\sigma^2) - \exp[-(J+1)^2/2\sigma^2]. \tag{3}$$

Here T is the nuclear temperature, E_0 is the pairing energy, and σ is the spin cutoff parameter. The parameters $T=2.6$ MeV, $E_0=-5.4$ MeV, and $\sigma=2.46$ were taken from the work by Egidy *et al.* [40]. The normalization constant c was adjusted to fulfill the condition $N(0)=1$. This theoretical estimate together with our experimental result is plotted in Fig. 4. The very good agreement up to the excitation energy 6.3 MeV for spins from 0 to 6 allows us to consider the level scheme to be complete or nearly complete in these energy and spin ranges.

IV. MECHANISM OF THE (n, γ) REACTION

The target nucleus ^{23}Na lies among the nuclei ^{12}C, ^{13}C, ^{28}Al, ^{31}P, ^{32}S, ^{33}S, and ^{34}S, for which contributions of direct capture of s-wave neutrons by $p_{3/2}$ and $p_{1/2}$ orbitals were reported (see Refs. [6,41–43]). Despite the relatively large thermal neutron cross section ($\sigma_\gamma=0.53$ b [45]), one could expect such a contribution also for ^{23}Na. Our new (n, γ) and (d, p) data allow us to investigate the role of the direct capture mechanism in the $^{23}\mathrm{Na}(n, \gamma)$ reaction.

According to Ref. [45], the partial direct capture cross section for odd target nuclei can be written as

$$\sigma_{\gamma f}^{DC} = \sum_i \sigma_{if} S_{if}^2, \tag{4}$$

where

$$S_{if}^2 = (2J_i+1)(2J_f+1)\left[2\begin{Bmatrix} 3/2 & 1/2 & 1 \\ J_i & J_f & J_t \end{Bmatrix} S_{3/2} - \sqrt{2}\begin{Bmatrix} 1/2 & 1/2 & 1 \\ J_i & J_f & J_t \end{Bmatrix} S_{1/2}\right]^2, \tag{5}$$

$$\sigma_{if} = \frac{0.062}{R\sqrt{E_n}}\left[\frac{Z}{A}\right]^2 \frac{Y_f^2}{6(2J_t+1)}\left[\frac{Y_f+3}{Y_f+1}\right]^2 \times\left[1 + \frac{R-a_i}{R}Y_f\frac{Y_f+2}{Y_f+3}\right]^2, \tag{6}$$

and

$$Y_f^2 = \frac{2mE_\gamma R^2}{\hbar^2}. \tag{7}$$

Here Z is the proton number, A is the atomic number, R is the interaction radius (usually taken in the form

$1.35A^{1/3}$ fm), a_i is the coherent scattering length for channel spin i corresponding to spins $J_i = J_t \pm 1/2$, J_f is the total spin of the final state, J_t is the spin of the target, $S_{1/2}$ and $S_{3/2}$ are the (d, p) spectroscopic amplitudes for the $p_{1/2}$ and $p_{3/2}$ components, E_γ is the energy of the primary γ transition, and E_n is the incident neutron energy (0.0253 eV for 2200 m/s neutrons). The free scattering coherent lengths $a_+ = 6.17$ fm and $a_- = -1.08$ fm were taken from the compilation [44].

The calculated values of the contributions of the direct capture mechanism are compared with our experimental partial cross sections in Table VI. The large difference between the calculated and experimental values can be attributed to the compound nucleus (CN) mechanism. However, taking into account only six levels with the highest spectroscopic factors from the (d, p) experiment (in Table VI these levels are printed in bold) one will obtain a striking high correlation between σ^{DC} and σ^{exp}. This correlation is documented by correlation coefficient $\varrho^{exp} = \varrho(\sigma_{\gamma f}^{exp}, \sigma^{DC}) = 0.997$. Such high correlation deserves our attention.

The partial cross section, incorporating both mechanisms, can be deduced from the generally accepted expression

$$\sigma_{\gamma f} = [\sqrt{\sigma_{\gamma f}^{DC}} + \eta\sqrt{\langle\sigma_{\gamma f}^{CN}\rangle}]^2, \tag{8}$$

which takes into account the Porter-Thomas fluctuations and where η is a realization of a random variable, subjected to normal distribution with a zero mean and a unit variance. To estimate $\langle\sigma_{\gamma f}^{CN}\rangle$ we assumed, as starting point, that $\sigma^{CN} = \sigma^{exp} - \Sigma_f\ \sigma_{\gamma f}^{DC}$, the ratio $\langle\sigma_{\gamma f}^{CN}\rangle/E_\gamma^3$ is constant and the ratio between $E1$ and $M1$ photon strengths is 7. Further, we used the value of 1% from the compilation [38] as the estimation of the contribution of the 2^+ initial channel to the total cross section of thermal neutron capture. The values of $\langle\sigma_{\gamma f}^{C} N\rangle$ estimated in this way are given in last column of Table VI. Performing a Monte Carlo calculation and using Eq. (8) we tested how compatible is $\varrho^{exp} = \varrho(\sigma_{\gamma f}^{exp}, \sigma_{\gamma f}^{DC}) = 0.997$ with the distribution of correlation distribution $\varrho^{MC} = \varrho(\sigma_{\gamma f}, \sigma^{DC})$. We obtained an average value of ϱ^{MC} to be $\langle\varrho^{MC}\rangle = 0.647$ and a probability for the occurrence of $\varrho^{MC} > \varrho^{exp}$ to be only $P(\varrho^{MC} > \varrho^{exp}) = 0.13\%$.

To be sure that this extremely small probability is not caused only by our assumptions mentioned above, we perform another test with other assumptions. We presupposed that the ratio $\langle\sigma_{\gamma f}^{CN}\rangle/E_\gamma^5$ is constant and that the ratio between $E1$ and $M1$ strengths is equal to 1. In addition, we multiplied $\sigma_{\gamma f}^{DC}$ from Table VI artificially by factor 3, increasing in this way the role of the compound nucleus. Even in this case we arrive at the very low probability for occurrence $\varrho^{MC} > \varrho^{exp}$, $P(\varrho^{MC} > \varrho^{exp}) = 1.7\%$.

This result could mean that generally accepted ideas about the CN mechanisms are not valid for levels which are significantly populated via the direct capture mechanisms. However, an unknown phase between $S_{1/2}$ and $S_{3/2}$ for the level at 4207 keV and an ambiguous spin for the level at 4196 keV do not allow us to state a more firm conclusion on the interplay of the direct capture and compound nucleus mechanisms. On the other hand, it should be noted that similar features were seen for the target nuclei ^{125}Te [46] and ^{126}Te [47].

V. CONCLUSIONS

Using the (n, γ) and the $(\vec{d}, p)$ reaction we constructed a complete level as well as decay scheme up to the excitation energy of 6.3 MeV. The spin-parity assignments are essentially complete up to 3.7 MeV. Above this, energy spin and parity become less reliable. These uncertainties could be converted into unique assignments comparing our spectroscopic results with modern model predictions for levels above 3.7 MeV. The very extensive spectroscopic information in our work could be challenging for tests of various theoretical approaches.

Although the ^{23}Na(n, γ) reaction is supposed to be dominated by a compound nucleus mechanism, we find extremely high correlation between the calculated direct capture contributions and the experimental values of the partial cross sections for the six levels with the highest spectroscopic strength. The rivalry of these two mechanisms deserves further investigation in other nuclei.

ACKNOWLEDGMENT

This work was supported by the DFG under Grant Nos. IIC4-Eg 25/4-1 and 436TSE17/2/97.

[1] J. Vernotte, G. Berrier-Ronsin, S. Fortier, W. Hourami, J. Kalifa, J. M. Kalifa, J. M. Maison, L.-H. Rosier, G. Rotbard, and B. H. Wildenthal, Phys. Rev. **57**, 1256 (1998).

[2] E. T. Jurney, J. W. Starner, J. E. Lynn, and S. Raman, Phys. Rev. C **56**, 118 (1997).

[3] S. Raman, E. K. Warburton, J. W. Starner, E. T. Jurney, J. E. Lynn, P. Tikkanen, and J. Keinonen, Phys. Rev. C **53**, 616 (1996).

[4] T. A. Walkiewicz, S. Raman, E. T. Jurney, J. W. Starner, and J. E. Lynn, Phys. Rev. C **45**, 1597 (1992).

[5] S. Raman, E. T. Jurney, J. W. Starner, and J. E. Lynn, Phys. Rev. C **46**, 972 (1992).

[6] S. Raman, R. F. Carlton, J. C. Wells, E. T. Jurney, and J. E. Lynn, Phys. Rev. C **32**, 18 (1985).

[7] P. M. Endt, Nucl. Phys. **A633**, 1 (1998); ENSDF compilation, world wide web http://ie.lbl.gov/ensdf

[8] G. A. Bartholomew, A. Doveika, K. M. Eastwood, S. Monaro, L. V. Groshev, A. M. Demidov, V. Pelkhov, and L. L. Sokolovskij, Nucl. Data, Sect. A **3**, 367 (1967).

[9] L. W. Nichol, A. H. Colenbrander, and T. J. Kennett, Can. J. Phys. **47**, 953 (1969).

[10] A. M. Wilson, H. J. Jackson, and G. E. Thomas, Nucl. Sci.

Eng. **63**, 55 (1977).
[11] T. A. A. Tielens, J. Kopecky, K. Abrahams, and P. M. Endt, Nucl. Phys. **A403**, 13 (1983).
[12] T. A. A. Tielens and J. B. M. De Haas, Nucl. Phys. **A425**, 303 (1984).
[13] P. Hungerford, T. von Egidy, H. H. Schmidt, S. A. Kerr, H. G. Börner, and E. Monnand, Z. Phys. A **313**, 325 (1983).
[14] Zhang Ming, Shi Zongren, Zeng Xiantang, Li Guohua, and Ding Dazhao, Chin. J. Nucl. Phys. **9**, 307 (1987).
[15] J. Hori, S. T. Park, S. Y. Lee, M. Igashira, and T. Ohsaki, J. Nucl. Sci. Technol. **38**, 91 (2001).
[16] D. F. H. Start, N. A. Jelley, J. Burde, D. A. Hutcheon, W. L. Randolph, B. Y. Underwood, and R. E. Warner, Nucl. Phys. **A206**, 207 (1973).
[17] P. Ekström, J. Tillman, and L. Carln, Nucl. Phys. **A210**, 458 (1973).
[18] P. J. M. Smulders, Nucl. Phys. **A210**, 579 (1973).
[19] A. S. Keverling Buismann and P. J. M. Smulders, Nucl. Phys. **A228**, 205 (1974).
[20] A. S. Keverling Buismann, Ph. B. Smith, P. J. M. Smulders, and H. Gruppelaar, Nucl. Phys. **A176**, 161 (1971).
[21] A. Sperduto and W. W. Buechner, Phys. Rev. **88**, 574 (1952).
[22] C. Daum, Nucl. Phys. **45**, 273 (1963).
[23] E. Krämer, G. Mairle, and G. Kaschl, Nucl. Phys. **A165**, 353 (1971).
[24] D. O. Boerma (unpublished); data in Ref. [7].
[25] R. J. Peterson, F. E. Cecil, R. A. Ristinen, E. R. Flynn, N. Stein, and J. D. Sherman, Phys. Rev. C **14**, 868 (1976).
[26] K. D. Singer, S. C. Headley, L. R. Medsker, and H. T. Fortune, Phys. Rev. C **15**, 1662 (1977).
[27] H. T. Fortune, L. R. Medsker, S. C. Headley, and K. D. Singer, J. Phys. G **4**, 1463 (1978).
[28] Y. Kadota, K. Ogino, K. Obori, Y. Taniguchi, T. Tanabe, M. Yasue, and J. Schmizu, Nucl. Phys. **A458**, 523 (1986).
[29] M. Löffler, H. J. Scheerer, and H. Vonach, Nucl. Instrum. Methods **111**, 1 (1973).
[30] E. Zanotti, M. Bisenberger, R. Hertenberger, H. Kader, and G. Graw, Nucl. Instrum. Methods Phys. Res. A **310**, 706 (1991).
[31] J. R. Comfort, code CHUCK3 (1980), version of CHUCK2 by P. D. Kunz (unpublished).
[32] C. Daum, Nucl. Phys. **45**, 273 (1963).
[33] C. M. Perey and P. G. Perey, At. Data Nucl. Data Tables **17**, 1 (1976).
[34] W. W. Daehnick, J. D. Childs, and Z. Vrcelj, Phys. Rev. C **21**, 2253 (1980).
[35] B. H. Wildenthal, Prog. Part. Nucl. Phys. **11**, 4 (1984).
[36] A. H. Wapstra, Nucl. Instrum. Methods Phys. Res. A **292**, 671 (1990).
[37] R. C. Greenwood and R. E. Chrien, Nucl. Instrum. Methods **175**, 515 (1980).
[38] *Neutron Cross Sections*, edited by S. F. Mughabghab, M. Divideenam, and N. E. Holden (Academic Press, New York, 1981), Vol. 1, Pt A.
[39] A. Gilbert and A. G. W. Cameron, Can. J. Phys. **43**, 1446 (1965).
[40] T. von Egidy, H. H. Schmidt, and A. N. Behkami, Nucl. Phys. **A481**, 189 (1988).
[41] S. F. Mughabghab, M. A. Lone, and B. C. Robertson, Phys. Rev. C **26**, 2698 (1982).
[42] Shi Zongren, Zeng Xiantang, and Guo Taicheng, Chin. J. Nucl. Phys. **4**, 88 (1982).
[43] R. L. Macklin and S. F. Mughabghab, Phys. Rev. C **32**, 379 (1985).
[44] L. Koester, H. Rauch, and E. Seymann, At. Data Nucl. Data Tables **49**, 65 (1991).
[45] *Neutron Cross Sections* (Ref. [38]), Vol. 1, Pt B.
[46] J. Honzátko, K. Konečný, and I. Tomandl, Czech. J. Phys. **44**, 11 (1994).
[47] J. Honzátko, K. Konečný, and F. Bečvář, Czech. J. Phys. **40**, 117 (1990).